Comput Visual Sci (2008) 11:41–58
DOI 10.1007/s00791-006-0056-3

REGULAR ARTICLE

Monotonicity preserving multigrid time stepping schemes for conservation laws

Justin W. L. Wan · Antony Jameson

Received: 10 January 2006 / Accepted: 26 June 2006 / Published online: 9 January 2007

Abstract In this paper, we propose monotonicity preserving and total variation diminishing (TVD) multigrid methods for solving scalar conservation laws. We generalize the upwind-biased residual restriction and interpolation operators for solving linear wave equations to nonlinear conservation laws. The idea is to define nonlinear restriction and interpolation based on local Riemann solutions. Theoretical analyses have been provided to analyze the monotonicity preserving and TVD properties of the resulting multigrid time stepping schemes. Numerical results are given to verify the theoretical results and demonstrate the effectiveness of the proposed schemes. Two dimensional extension is also discussed.

1 Introduction

Multigrid has shown to be a powerful and one of the most efficient numerical techniques for solving elliptic partial differential equations (PDEs) [3,13,33]; its convergence rate is often independent of the mesh size. Well established convergence theory, [2,13,35] and sophisticated smoothing, [3,32–34], coarsening, [5,6,30], and interpolation [1,4,28,29,36] techniques have been developed. However, the fundamental study of multigrid for hyperbolic equations is far less well-developed. One major difficulty is that the discretization matrices of hyperbolic equations are in general nonsymmetric, and hence the smoothing property of relaxation methods, and the minimization property of Galerkin coarse grid correction, both of which are essentially based on symmetry and positive definiteness, may not hold anymore for hyperbolic equations. If the multigrid principle of reducing the high and low frequency errors reflects the smoothing nature of elliptic operators, then the intrinsic wave propagation nature of hyperbolic equations must also be reflected in the hyperbolic multigrid methods. The objective of this paper is to study and analyze the wave propagation property of specially designed monotonicity preserving multigrid time stepping methods.

Multigrid methods for hyperbolic equations, in particular, steady Euler equations, are first proposed by Ni [27] and Jameson [18]. In their approach, the key is to accelerate wave propagation on multiple grids since larger time steps can be taken on coarse grids without violating the CFL condition. Thus, the low frequency disturbances are rapidly expelled through the outer boundary whereas the high frequency errors are locally damped. Multigrid time stepping schemes exploiting this effect have also been proposed in [14,15]. Since then, a great deal of progress has been made in this direction; see the references in the survey paper by Hemker and Johnson [16].

The fast wave propagation argument was made more precise by Jespersen [20] who showed that, under certain assumptions, such multigrid time stepping schemes on M-grid are consistent and first order accurate, with effective time step, $\Delta t = \sum_k^M \Delta t_k$, where Δt_k is the time step taken on grid k. Gustafsson and Lötstedt [12,24]

Communicated by P. Wesseling.

J. W. L. Wan (✉)
School of Computer Science, University of Waterloo,
Waterloo, ON N2L 3G1, Canada
e-mail: jwlwan@cs.uwaterloo.ca

A. Jameson
Department of Aeronautics and Astronautics,
Stanford University, Stanford, CA 94305-4035, USA

also proved using Fourier analysis that the speed of the *smooth* wave propagation is $2^M - 1$, assuming the mesh size is double on each coarse grid. The results of Jespersen addressed the issue of consistency; the analysis in this paper, on the other hand, addresses the issue of stability–monotonicity preserving and total variation diminishing.

We note that although the main purpose is to rapidly expell the low frequency disturbances out of the boundary, it turns out that numerical oscillations can delay the propagation substantially. As an example, we apply a three-level multigrid with Jacobi smoothing, linear interpolation, and Galerkin coarse grid correction to solve an 1D linear wave equation. The initial condition (disturbance) is a square wave. The numerical solution in the subsequent multigrid cycles are shown in Fig. 1. By the analysis of Gustafsson and Lötstedt, the three-level multigrid should have converged in $128/7 \approx 18$ multigrid cycles. Instead, it requires more than 80 cycles to convergence due to the spurious oscillations generated at the tail of the square wave. Thus, it is imperative to design nonoscillatory multigrid algorithms.

In [17], Jameson proposed two multigrid time stepping schemes for the steady state solution of the one-dimensional linear wave equation. The idea is based on an upwind biased interpolation and residual restriction operators, which capture the characteristics of the underlying PDE, and a modified coarse grid update

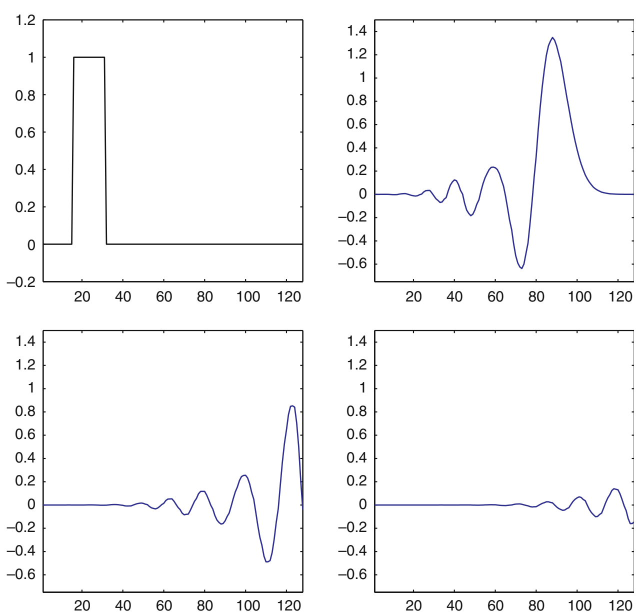

Fig. 1 The numerical solution given by a three-level multigrid at **a** time step = 0, **b** time step = 20, **c** time step = 40, **d** time step = 60

formula. He proved that, for two-level, these schemes preserve monotonicity. In this paper, we extend the analysis to the multilevel case, and in addition, prove the total variation diminishing (TVD) property. Furthermore, we propose and analyze an extension to nonlinear conservation laws. For nonlinear equations, the additional challenge is that we also have to capture discontinuities arising from shocks, and rarefactions without violating the entropy conditions. As Riemann solutions for nonlinear hyperbolic equations are the counterparts of characteristics for linear equations, our key idea of constructing nonlinear upwind interpolation is based on solving local Riemann problems. The analysis of the linear and nonlinear multigrid time stepping schemes will be focused on the monotonicity preserving and the TVD properties which have never been studied in the context of multigrid. Nevertheless, these properties are essential to obtain nonoscillatory schemes. Using these requirements as design tools, it is hoped that it will bring new insight into the design of efficient hyperbolic multigrid methods.

Further algorithmic improvements of the fast wave propagation on multiple grids approach have been developed. In [21], Koren and Hemker used an upwind prolongation, and the restriction essentially is the adjoint of the prolongation. A similar prolongation and restriction technique based on characteristics is used by LeClercq and Stoufflet [22] for unstructured grid computations. Grasso and Marini [11] derived another upwind prolongation based on MUSCL reconstruction for solving Navier-Stokes equations. Ferm and Lötstedt [9] used a residual dependent restriction for handling shocks when solving Burgers' equation. Different relaxation smoothings are compared in [26] for solving the one-dimensional Burgers' equation. Mulder [25] proposed the use of multiple semi-coarsening to handle anisotropic PDE coefficients arising from the alignment of flow with the grid. Eliasson [7] considered the use of higher order transfer operators to maintain stability of the coarse grid problem. Spekreijse [31] proposed a multigrid scheme for a monotone second order discretization of hyperbolic conservation laws.

In Sect. 2, we describe the multiplicative and additive schemes proposed by Jameson for solving the linear wave equations, and in Sect. 3, our generalization to nonlinear conservation laws. In Sect. 4, we present a multilevel analysis on the monotonicity preserving and TVD properties of the linear multigrid schemes, and in Sect. 5, a two-level analysis for the proposed nonlinear multigrid scheme. Finally, numerical results are presented in Sect. 6 to demonstrate their effectiveness of accelerating wave propagation on multiple grids; a two-dimensional example is also given.

2 Linear wave equation

Since our nonlinear multigrid time stepping schemes are built upon the linear schemes, we first describe the linear case in details, followed by the nonlinear case. The model linear wave equation in one dimension is:

$$\begin{aligned} &u_t + u_x = 0 \quad 0 < x < 1, \\ &u(0,t) = 0, \quad u(x,0) = u_0(x). \end{aligned} \tag{1}$$

We are interested in the steady state solution which, in this case, is $u \equiv 0$. We discretize the equation by the standard first order upwind scheme:

$$u_j^{n+1} = u_j^n - \lambda \left(u_j^n - u_{j-1}^n \right), \tag{2}$$

where $\lambda = \Delta t^h / \Delta x^h$ is the CFL number. If a single grid with N grid points is used, it will take N/λ time steps to march to the steady state. The objective is to accelerate propagation on multiple grids while preserving monotonicity and being TVD for $\lambda \leq 1$.

Given a fine grid $\{x_j^h\}, j = 0, 1, 2, \ldots, N$, the grid points with even indices are selected as coarse grid points $\{x_j^H\}$, $j = 0, 2, 4, \ldots, N$. The superscripts h and H denote functions on the fine and coarse grids, respectively, whereas the subscript j denotes the corresponding jth grid point. In a standard two-level algorithm (FAS-cycle for nonlinear equations) [3,16], we start with the current approximation u^n, and the update u^{n+1} is obtained by

$$\begin{aligned}
&\text{upwind smoothing:} && \bar{u}_j^h = u_j^n - \lambda \left(u_j^n - u_{j-1}^n \right) \\
&\text{fine grid residual:} && \bar{r}_j^h = \tfrac{1}{\Delta x^h} \left(\bar{u}_j^h - \bar{u}_{j-1}^h \right) \\
&\text{restriction of } \bar{u}^h\text{:} && u_{2j}^H = \mathcal{R}_u \bar{u}_{2j}^h \\
&\text{coarse grid RHS:} && b_{2j}^H = \tfrac{1}{\Delta x^H} \left(u_{2j}^H - u_{2j-2}^H \right) \\
& && \qquad - \mathcal{R}_r \bar{r}_{2j}^h \\
&\text{coarse grid evolution:} && \bar{u}_{2j}^H = u_{2j}^H - \lambda \left(u_{2j}^H - u_{2j-2}^H \right) \\
& && \qquad + \Delta t^H b_{2j}^H.
\end{aligned}$$

Here, $\mathcal{R}_u$ and $\mathcal{R}_r$ denote the solution and residual restriction operators, respectively. Finally, we interpolate the coarse grid error to the fine grid and obtain:

$$u^{n+1} = \bar{u}^h + \mathcal{P} \left(\bar{u}^H - \mathcal{R}_u \bar{u}^h \right), \tag{3}$$

where $\mathcal{P}$ is the interpolation operator. As shown by the previous example, simple choices such as linear interpolation may lead to poor convergence due to severe numerical oscillations. In the next sections, we describe an upwind restriction and interpolation, and a modified coarse grid update formula.

2.1 Upwind restriction and interpolation

To define a conservative restriction operator, the upwind-biased residual restriction[17] is defined as the following averaging operator:

$$\mathcal{R}_r \bar{r}_j^h = \frac{1}{2} (\bar{r}_j^h + \bar{r}_{j-1}^h), \tag{4}$$

since the characteristics are from left to right; see Fig. 2a. This idea is essentially the same as the upwind schemes. Similarly, the interpolation of a coarse grid function v^H is given by:

$$(\mathcal{P} v^H)_{2i} = (\mathcal{P} v^H)_{2i+1} = v_{2i}^H, \tag{5}$$

which predicts information to the right; see Fig. 2b. We note that interpolations based on characteristics have also been used in [21,22].

2.2 Higher order interpolation

It is observed that the use of linear interpolation will, in fact, lead to oscillations. Fig. 3 shows the discrete functions u^n, $\bar{u}^h$, etc, as defined in Sect. 2. The current

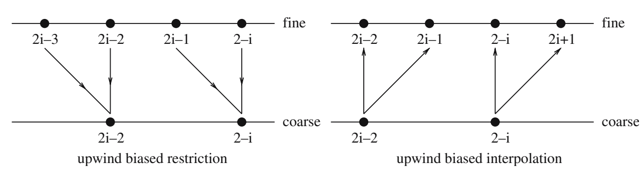

Fig. 2 **a** Upwind biased restriction **b** Upwind biased interpolation

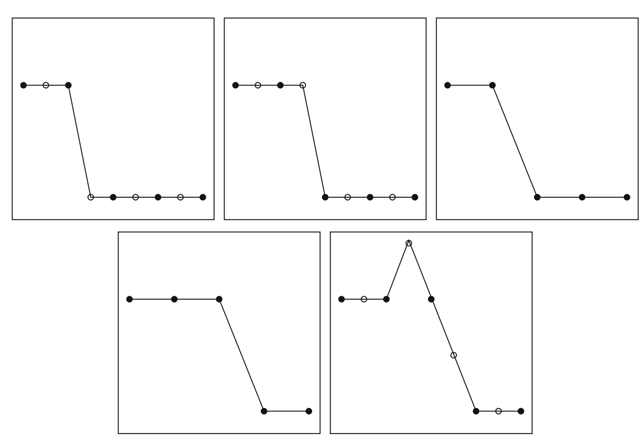

Fig. 3 Oscillation caused by linear interpolation. From *left* to *right*, *top* to *bottom*: u^n, $\bar{u}^h$, u^H, $\bar{u}^H$, and u^{n+1}. The *black dots* denote coarse grid points

approximation u^n is defined as:

$$u_j^n = \begin{cases} 1 & j = 0, 1, 2. \\ 0 & j = 3, 4, \ldots, 8. \end{cases}$$

The functions $\bar{u}^h$, u^H, and $\bar{u}^H$ are computed based on the two-level algorithm with $\lambda = 1$. In the final step, we see that overshoot occurs at u_3^{n+1}: by (3),

$$\begin{aligned} u_3^{n+1} &= \bar{u}_3^h + \mathcal{P}_{\text{linear}} \left(\bar{u}^H - u^H \right)_3 \\ &= \bar{u}_3^h + \frac{\bar{u}_2^H + \bar{u}_4^H}{2} - \frac{u_2^H + u_4^H}{2} = \frac{3}{2}. \end{aligned}$$

As for comparisons, if the upwind biased interpolation is used, then

$$\begin{aligned} u_3^{n+1} &= \bar{u}_3^h + \mathcal{P}_{\text{upwind}} \left(\bar{u}^{n+1} - u^H \right)_3 \\ &= \bar{u}_3^h + \bar{u}_2^H - u_2^H = 1. \end{aligned}$$

See also Fig. 4.

2.3 Coarse grid update

It is further observed that even with the use of upwind restriction and interpolation, oscillations can still occur. Figure 5 shows a similar sequence of plots as in Fig. 3 with slightly different u^n. This time, undershoot occurs at u_3^{n+1}. To fix this, a new update formula [17] is used:

$$u^{n+1} = \bar{u}^h + \mathcal{P} \left(\bar{u}^H - \mathcal{R}_u u^n \right).$$

The idea is to compute the coarse grid error by the difference of the coarse grid evolved solution $\bar{u}^H$ and the restriction of the original function u^n, instead of $\bar{u}^h$. As shown in Fig. 6, the oscillation is eliminated.

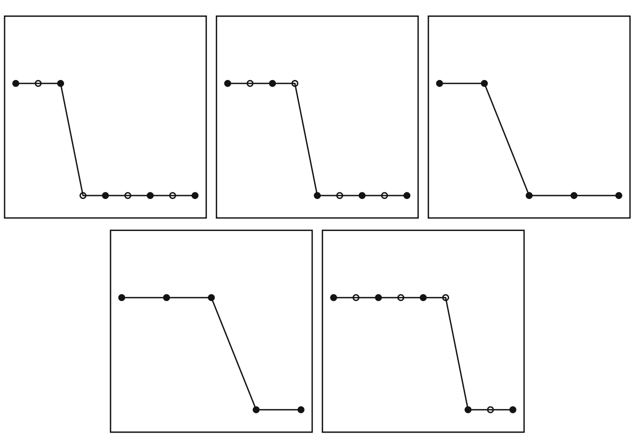

Fig. 4 No oscillation using upwind interpolation. From *left* to *right*, *top* to *bottom*: u^n, $\bar{u}^h$, u^H, $\bar{u}^H$, and u^{n+1}

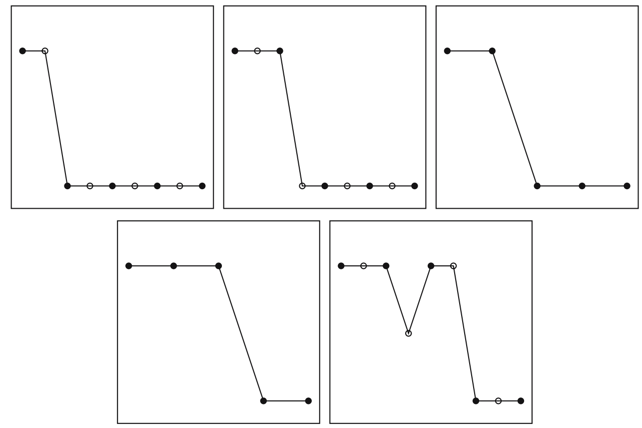

Fig. 5 Oscillation caused by standard update. From *left* to *right*, *top* to *bottom*: u^n, $\bar{u}^h$, u^H, $\bar{u}^H$, and u^{n+1}.

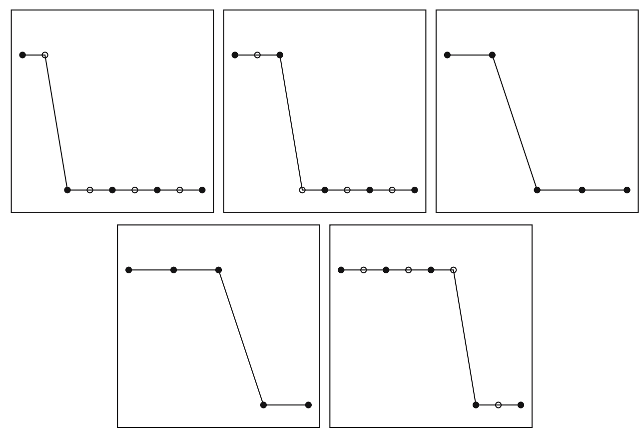

Fig. 6 No oscillation using the new coarse grid update formula. From *left* to *right*, *top* to *bottom*: u^n, $\bar{u}^h$, u^H, $\bar{u}^H$, and u^{n+1}

2.4 Algorithms

Before we present the algorithms, we note that the forcing term on the coarse grid, b_j^H, can be simplified as follows:

$$\begin{aligned} b_j^H &\equiv \frac{1}{\Delta x^H} \left(u_j^H - u_{j-2}^H \right) - \frac{1}{2} \left(\bar{r}_j^h + \bar{r}_{j-1}^h \right) \\ &= \frac{1}{2\Delta x^h} \left(\bar{u}_j^h - \bar{u}_{j-2}^h \right) - \frac{1}{2\Delta x^h} \left[\left(\bar{u}_j^h - \bar{u}_{j-1}^h \right) \right. \\ &\quad \left. + \left(\bar{u}_{j-1}^h - \bar{u}_{j-2}^h \right) \right] \\ &= 0. \end{aligned}$$

Once the two-level scheme is defined, the multilevel scheme can be obtained from applying the two-level algorithm recursively on the coarser grids. We denote functions on the first grid, which is also the finest grid, by superscript (1); the second grid by (2), and so on. The multilevel multigrid time stepping scheme is:

Algorithm: Linear Multiplicative Scheme

$u^{(1)} = u^n$
Define $\tilde{u}^{(k)}$=$\mathrm{MG}^{\mathrm{Mult}}_{\mathrm{linear}}(u^{(k)})$ by:
 if $k = L$,
 $$\tilde{u}^{(k)}_j = u^{(k)}_j - \lambda\left(u^{(k)}_j - u^{(k)}_{j-2^{k-1}}\right) \quad (j = 0, 2^{k-1}, 2\cdot 2^{k-1}, \ldots.)$$
 else
 $$\bar{u}^{(k)}_j = u^{(k)}_j - \lambda\left(u^{(k)}_j - u^{(k)}_{j-2^{k-1}}\right) \quad (j = 0, 2^{k-1}, 2\cdot 2^{k-1}, \ldots.)$$
 $$u^{(k+1)}_j = \bar{u}^{(k)}_j \quad (j = 0, 2^{k}, 2\cdot 2^{k}, \ldots.)$$
 $\tilde{u}^{(k+1)}$=$\mathrm{MG}^{\mathrm{Mult}}_{\mathrm{linear}}(u^{(k+1)})$
 $$\tilde{u}^{(k)}_j = \tilde{u}^{(k+1)}_j \quad (j = 0, 2^{k}, 2\cdot 2^{k}, \ldots.)$$
 $$\tilde{u}^{(k)}_{j-2^{k-1}} = \bar{u}^{(k)}_{j-2^{k-1}} + \bar{u}^{(k+1)}_{j-2^k} - u^{(k)}_{j-2^k} \quad (j = 0, 2^{k}, 2\cdot 2^{k}, \ldots.)$$
 end
$u^{n+1} = \mathrm{MG}^{\mathrm{Mult}}_{\mathrm{linear}}(u^{(1)})$

Since on each coarse grid k, we use the most update information $\bar{u}^{k-1}$ from the finer grid, this method is called the multiplicative scheme. If we restrict and propagate u^n on all the coarse grids, the resulting algorithm is called the additive scheme:

Algorithm: Linear Additive Scheme

$u^{(1)} = u^n$
Define $\tilde{u}^{(k)}$=$\mathrm{MG}^{\mathrm{Add}}_{\mathrm{linear}}(u^{(k)})$ by:
 if $k = L$,
 $$\tilde{u}^{(k)}_j = u^{(k)}_j - \lambda\left(u^{(k)}_j - u^{(k)}_{j-2^{k-1}}\right) \quad (j = 0, 2^{k-1}, 2\cdot 2^{k-1}, \ldots.)$$
 else
 $$\bar{u}^{(k)}_j = u^{(k)}_j - \lambda\left(u^{(k)}_j - u^{(k)}_{j-2^{k-1}}\right) \quad (j = 0, 2^{k-1}, 2\cdot 2^{k-1}, \ldots.)$$
 $$u^{(k+1)}_j = u^{(k)}_j \quad (j = 0, 2^{k}, 2\cdot 2^{k}, \ldots.)$$
 $\tilde{u}^{(k+1)}$=$\mathrm{MG}^{\mathrm{Add}}_{\mathrm{linear}}(u^{(k+1)})$
 $$\tilde{u}^{(k)}_j = \tilde{u}^{(k+1)}_j \quad (j = 0, 2^{k}, 2\cdot 2^{k}, \ldots.)$$
 $$\tilde{u}^{(k)}_{j-2^{k-1}} = \bar{u}^{(k)}_{j-2^{k-1}} + \bar{u}^{(k+1)}_{j-2^k} - u^{n}_{j-2^k} \quad (j = 0, 2^{k}, 2\cdot 2^{k}, \ldots.)$$
 end
$u^{n+1} = \mathrm{MG}^{\mathrm{Add}}_{\mathrm{linear}}(u^{(1)})$

Remark The wave propagation by the multiplicative scheme is generally twice as fast as the additive scheme (cf. Gauss-Seidel vs. Jacobi).

3 Nonlinear conservation laws

In this section, we generalize the methodology for linear wave equations to nonlinear equations. We consider the model scalar conservation law in one dimension:

$$u_t + f(u)_x = 0 \quad 0 < x < 1, \tag{6}$$

with appropriate boundary and initial conditions. The flux $f(u)$ is assumed to be convex. Again, we are interested in obtaining the steady state solution fast.

We discretize the equations by the EO scheme [8]:

$$u^{n+1}_j = u^n_j - \lambda\left(F^{EO}\left(u^n_j, u^n_{j+1}\right) - F^{EO}\left(u^n_{j-1}, u^n_j\right)\right). \tag{7}$$

The numerical flux F^{EO} is defined as

$$F^{EO}(u_L, u_R) = \frac{1}{2}(u^+_L)^2 + \frac{1}{2}(u^-_R)^2,$$

where $u^+ \equiv \max(u, 0)$ and $u^- \equiv \min(u, 0)$. We note that the first order EO scheme is used for illustration purpose only; other schemes such as Godunov [10] or more sophisticated high resolution schemes [23] can be used as well.

The basic principle of the multigrid time stepping schemes, either multiplicative or additive, is essentially unchanged even in the nonlinear case; we smooth or propagate the wave on the fine grid, and accelerate the propagation on the coarse grids. We need, however, to make several modifications. For instance, the upwinding smoothing (2) is now substituted by the EO smoothing (7). The restriction and interpolation require more detail explanations which are described in the next section.

3.1 Nonlinear upwind restriction and interpolation

In the linear case, the characteristics are constantly from left to right at each grid point, and hence the upwind restriction and interpolation can be determined a priori by (4) and (5). For nonlinear conservation laws, however, the characteristics depend on the current solution, and the characteristic directions change from grid points to grid points. Furthermore, shocks and rarefaction waves can occur anywhere. Hence, we need to devise a simple and yet accurate mechanism to determine whether the coarse grid point should interpolate (restrict) to the left or to the right, and more importantly, how to handle shocks and rarefactions. Since restriction and interpolation are essentially based on the same principle, we shall describe the interpolation only.

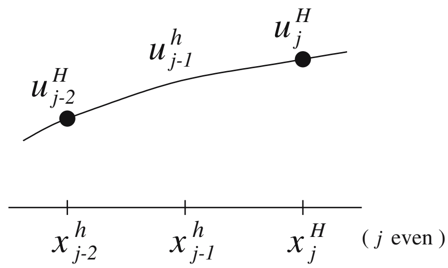

Fig. 7 The interpolation value at the noncoarse grid point x^h_{j-1} is given by the solution of a local PDE problem for the linear wave equation, and the Riemann solution for the conservation law

Consider a two-level method. As shown in Fig. 7, for j even, given the coarse grid values u^H_{j-2} and u^H_j at the coarse grid points x^h_{j-2} and x^h_j, respectively, which value should we select at the fine grid point x^h_{j-1}? If both $f'(u^H_{j-2})$ and $f'(u^H_j)$ are positive (negative), the wave propagates to the right (left) locally and it resembles the linear case. Thus, we simply take u^H_{j-2} (u^H_j) for the value at x^h_{j-1}. When $f'(u^H_{j-2})$ is positive and $f'(u^H_j)$ is negative, i.e. a shock, we have information coming from both sides. Now, which one should we take? Either one, or the average of them? In the opposite case, when $f'(u^H_{j-2})$ is negative and $f'(u^H_j)$ is positive, rarefaction occurs. This situation seems even worse since the information is now going away.

Our idea is motivated by the following key observation. We view the problem shown in Fig. 7 as a local two-point boundary value problem. For the linear wave equation (one boundary value is in fact redundant), it can be written as:

$$u_t + u_x = 0 \quad x^H_{j-2} < x < x^H_j$$
$$u(x^h_{j-2}, t) = u^H_{j-2}, \quad u(x,0) = \bar{u}^h.$$

We then define the interpolation value at x^h_{j-1} as the steady state solution of the local two-point boundary value problem. Such interpolation is precisely the upwind biased interpolation described in Sect. 2.1. In other words, the upwind biased interpolation can be interpreted as solving local boundary value problems.

Generalizing this idea to conservation laws, we solve a local Riemann problem instead:

$$u_t + f(u)_x = 0$$
$$u(x,0) = \begin{cases} u^H_{j-2} & x^H_{j-2} < x < x^h_{j-1} \\ u^H_j & x^h_{j-1} < x < x^H_j. \end{cases}$$

Then, the interpolation value u^h_{j-1} is given by the Riemann solution. More precisely, if $f'(u^H_{j-2}) > f'(u^H_j)$, a shock occurs with speed, $s = \left(f(u^H_{j-2}) - f(u^H_j)\right)/(u^H_{j-2} - u^H_j)$. If $s \geq 0$, then $u^h_{j-1} = u^H_{j-2}$; if $s < 0$, then $u^h_{j-1} = u^H_j$. If $f'(u^H_{j-2}) < f'(u^H_j)$, it is a rarefaction wave. If they are of the same sign, then $u^h_{j-1} = u^H_{j-2}$ if they are positive, and $u^h_{j-1} = u^H_j$ if they are negative. Finally, if $u^H_{j-2} < 0 < u^H_j$, then the rarefaction wave turns out to be zero at x^h_{j-1} and hence $u^h_{j-1} = 0$.

Applying the Riemann solutions to the multilevel multiplicative scheme, the interpolation value $\tilde{u}^{(k)}_{j-2^{k-1}}$ is defined as:

$$\text{if } f'\left(\bar{u}^{(k)}_{j-2^k}\right) \geq 0, \quad f'\left(\bar{u}^{(k)}_j\right) \geq 0,$$
$$\tilde{u}^{(k)}_{j-2^{k-1}} = \bar{u}^{(k)}_{j-2^{k-1}} + \bar{u}^{(k+1)}_{j-2^k} - u^{(k+1)}_{j-2^k}$$
$$\text{if } f'\left(\bar{u}^{(k)}_{j-2^k}\right) \leq 0, \quad f'\left(\bar{u}^{(k)}_j\right) \leq 0,$$
$$\tilde{u}^{(k)}_{j-2^{k-1}} = \bar{u}^{(k)}_{j-2^{k-1}} + \bar{u}^{(k+1)}_j - u^{(k+1)}_j$$
$$\text{if } f'\left(\bar{u}^{(k)}_{j-2^{k-1}}\right) \geq 0 \geq f'\left(\bar{u}^{(k)}_j\right),$$
$$\tilde{u}^{(k)}_{j-2^{k-1}} = \begin{cases} u^+ & \text{if } f'\left(\bar{u}^{(k)}_{j-2^{k-1}}\right) \geq 0 \\ u^- & \text{if } f'\left(\bar{u}^{(k)}_{j-2^{k-1}}\right) < 0 \end{cases}$$
$$u^+ = \bar{u}^{(k)}_{j-2^{k-1}} + \bar{u}^{(k+1)}_{j-2^k} - u^{(k+1)}_{j-2^k},$$
$$u^- = \bar{u}^{(k)}_{j-2^{k-1}} + \bar{u}^{(k+1)}_j - u^{(k+1)}_j$$
$$\text{if } f'\left(\bar{u}^{(k)}_{j-2^k}\right) < 0 < f'\left(\bar{u}^{(k)}_j\right),$$
$$\tilde{u}^{(k)}_{j-2^{k-1}} = \bar{u}^{(k)}_{j-2^{k-1}}.$$

For the additive scheme, the interpolation is similar: $f'(\bar{u}^{(k)}_{j-2^k}), f'(\bar{u}^{(k)}_{j-2^{k-1}}), f'(\bar{u}^{(k)}_j)$ are substituted by $f'(u^n_{j-2^k})$, $f'(u^n_{j-2^{k-1}})$, $f'(u^n_j)$, and $u^{(k+1)}_{j-2^k}$, $u^{(k+1)}_j$ by $u^n_{j-2^k}$, u^n_j, respectively.

We remark that constructing interpolation by solving local linear boundary value problem has been used in multigrid methods for elliptic and convection-diffusion equations [13,33] as well as for hypersonic flow computations [21] in which the P-variant of Osher's approximate Riemann solver was used.

3.2 Algorithms

For the linear case, the forcing term $b^{(k)}_j \equiv 0$ for all j and k. In general, however, $b^{(k)}_j \neq 0$, and we need to include it in the algorithm. Denote the nonlinear upwind restriction and interpolation defined in Sect. 3.1 by $\mathcal{R}_{nl}$ and $\mathcal{P}_{nl}$, respectively. Define the residual of $u^{(k)}_j$ as:

$$r^{(k)}_j = \frac{1}{\Delta x^{(k)}}\left(F^{EO}\left(u^{(k)}_j, u^{(k)}_{j+2^{k-1}}\right) - F^{EO}\left(u^{(k)}_{j-2^{k-1}}, u^{(k)}_j\right)\right),$$

and similarly for the residual of $\bar{u}_j^{(k)}$. The nonlinear multilevel multiplicative and additive algorithms are given as follows:

Algorithm: Nonlinear Multiplicative Scheme

$u^{(1)} = u^n, b^{(1)} = 0$
Define $\tilde{u}^{(k)} = \mathrm{MG}^{\mathrm{Mult}}_{\mathrm{nonlinear}}(u^{(k)}, b^{(k)})$ by:
if $k = L$,
$$\tilde{u}_j^{(k)} = u_j^{(k)} - \Delta t^{(k)} r_j^{(k)} + \Delta t^{(k)} b_j^{(k)} \quad (j = 0, 2^{k-1}, 2 \cdot 2^{k-1}, \ldots.)$$
else
$$\bar{u}_j^{(k)} = u_j^{(k)} - \Delta t^{(k)} r_j^{(k)} + \Delta t^{(k)} b_j^{(k)} \quad (j = 0, 2^{k-1}, 2 \cdot 2^{k-1}, \ldots.)$$
$$u_j^{(k+1)} = \bar{u}_j^{(k)} \quad (j = 0, 2^k, 2 \cdot 2^k, \ldots.)$$
$$b_j^{(k+1)} = r_j^{(k+1)} - \mathcal{R}_{nl}\, \bar{r}_j^{(k)} \quad (j = 0, 2^k, 2 \cdot 2^k, \ldots.)$$
$$\tilde{u}^{(k+1)} = \mathrm{MG}^{\mathrm{Mult}}_{\mathrm{nonlinear}}(u^{(k+1)}, b^{(k+1)})$$
$$\tilde{u}_j^{(k)} = \tilde{u}_j^{(k+1)} \quad (j = 0, 2^k, 2 \cdot 2^k, \ldots.)$$
$$\tilde{u}_{j-2^{k-1}}^{(k)} = \bar{u}_{j-2^{k-1}}^{(k)} + \mathcal{P}_{nl}\, \left(\bar{u}^{(k+1)} - u^{(k)}\right)_{j-2^{k-1}} \quad (j = 0, 2^k, 2 \cdot 2^k, \ldots.)$$
end
$u^{n+1} = \mathrm{MG}^{\mathrm{Mult}}_{\mathrm{nonlinear}}(u^{(1)}, b^{(1)})$

Algorithm: Nonlinear Additive Scheme

$u^{(1)} = u^n, b^{(1)} = 0$
Define $\tilde{u}^{(k)} = \mathrm{MG}^{\mathrm{Add}}_{\mathrm{nonlinear}}(u^{(k)}, b^{(k)})$ by:
if $k = L$,
$$\tilde{u}_j^{(k)} = u_j^{(k)} - \Delta t^{(k)} r_j^{(k)} + \Delta t^{(k)} b_j^{(k)} \quad (j = 0, 2^{k-1}, 2 \cdot 2^{k-1}, \ldots.)$$
else
$$\bar{u}_j^{(k)} = u_j^{(k)} - \Delta t^{(k)} r_j^{(k)} + \Delta t^{(k)} b_j^{(k)} \quad (j = 0, 2^{k-1}, 2 \cdot 2^{k-1}, \ldots.)$$
$$u_j^{(k+1)} = u_j^{(k)} \quad (j = 0, 2^k, 2 \cdot 2^k, \ldots.)$$
$$b_j^{(k+1)} = r_j^{(k+1)} - \mathcal{R}_{nl}\, \bar{r}_j^{(k)} \quad (j = 0, 2^k, 2 \cdot 2^k, \ldots.)$$
$$\tilde{u}^{(k+1)} = \mathrm{MG}^{\mathrm{Add}}_{\mathrm{nonlinear}}(u^{(k+1)}, b^{(k+1)})$$
$$\tilde{u}_j^{(k)} = \tilde{u}_j^{(k+1)} \quad (j = 0, 2^k, 2 \cdot 2^k, \ldots.)$$
$$\tilde{u}_{j-2^{k-1}}^{(k)} = \bar{u}_{j-2^{k-1}}^{(k)} + \mathcal{P}_{nl}\, \left(\bar{u}^{(k+1)} - u^{(k)}\right)_{j-2^{k-2}} \quad (j = 0, 2^k, 2 \cdot 2^k, \ldots.)$$
end
$u^{n+1} = \mathrm{MG}^{\mathrm{Add}}_{\mathrm{nonlinear}}(u^{(1)}, b^{(1)})$

4 Linear analysis

In this section, we analyze the linear multigrid time stepping schemes described in Sect. 2.4 for the linear wave equation in one dimension. We shall provide a theoretical foundation for the upwind biased interpolation and restriction, and the modified coarse grid update which aim at minimizing numerical oscillations. Like discretization schemes for conservation laws, one important measure of nonoscillatory schemes is whether it preserves monotonicity. More precisely, if u^n is a nonincreasing (nondecreasing) function, after one time stepping (in our case, one multigrid cycle), u^{n+1} must remain nonincreasing (nondecreasing). Another important measure is total variation diminishing (TVD), which requires that the total variation of u^{n+1} does not exceed that of u^n. Both concepts are fundamental to designing numerical schemes for conservation laws, but nevertheless, have never been used to analyze multigrid methods.

Hence, the primary focus of our analysis is on the monotonicity and total variation diminishing properties of the MG time stepping schemes. In particular, we prove that both the two-level multiplicative and additive schemes preserve monotonicity and are TVD; and the same holds for multilevel additive scheme. In the following section, we analyze the convergence and speed of propagation by means of Fourier transform.

We first summarize the two-level case result here [17].

Theorem 4.1 *Both two-level multiplicative and additive multigrid time stepping schemes preserve monotonicity.*

Proof For j even, from the multiplicative algorithm,

$$u_j^{n+1} = \tilde{u}_j^h = \bar{u}_j^H = \bar{u}_j^h - \lambda\left(\bar{u}_j^h - \bar{u}_{j-2}^h\right),$$
$$u_{j-1}^{n+1} = \tilde{u}_{j-1}^h = \bar{u}_{j-1}^h + \bar{u}_{j-2}^H - u_{j-2}^n.$$

Subtracting the two and by direct computation,

$$\begin{aligned} &u_j^{n+1} - u_{j-1}^{n+1} \\ &\quad = (1-\lambda)^2\left(u_j^n - u_{j-1}^n\right) + 2\lambda(1-\lambda)\left(u_{j-2}^n - u_{j-3}^n\right) \\ &\qquad + \lambda\left(u_{j-3}^n - u_{j-4}^n\right) + \lambda^2(u_{j-4}^n - u_{j-5}^n). \end{aligned} \tag{8}$$

Similarly, for $j-1$ being odd, we have,

$$\begin{aligned} u_{j-1}^{n+1} - u_{j-2}^{n+1} &= \bar{u}_{j-1}^h + \bar{u}_{j-2}^H - u_{j-2}^n - \bar{u}_{j-2}^H \\ &= (1-\lambda)\left(u_{j-1}^n - u_{j-2}^n\right). \end{aligned} \tag{9}$$

Thus, if u^n is monotone, so is u^{n+1}, provided $0 \le \lambda \le 1$ satisfies the CFL condition.

For the additive scheme, the calculations are similar. For even j, we have

$$u_j^{n+1} = \tilde{u}_j^h = \bar{u}_j^H = u_j^n - \lambda\left(u_j^n - u_{j-2}^n\right),$$
$$u_{j-1}^{n+1} = \tilde{u}_{j-1}^h = \bar{u}_{j-1}^h + \bar{u}_{j-2}^H - u_{j-2}^n.$$

After simplifying,

$$u_j^{n+1} - u_{j-1}^{n+1} = (1-\lambda)\left(u_j^n - u_{j-1}^n\right) + \lambda\left(u_{j-2}^n - u_{j-3}^n\right) + \lambda\left(u_{j-3}^n - u_{j-4}^n\right), \tag{10}$$
$$u_{j-1}^{n+1} - u_{j-2}^{n+1} = (1-\lambda)\left(u_{j-1}^n - u_{j-2}^n\right). \tag{11}$$

Therefore, monotonicity is preserved for $0 \le \lambda \le 1$.

We generalize the above results to show that these two schemes are also TVD.

Theorem 4.2 *The two-level multiplicative and additive multigrid time stepping schemes are TVD.*

Proof Denote the total variation of a function u by $\mathrm{TV}(u)$. For the multiplicative scheme, using the formulae in (8) and (9),

$$\begin{aligned}
&\mathrm{TV}(u^{n+1})\\
&= \sum_j |u_j^{n+1} - u_{j-1}^{n+1}|\\
&= \sum_{\text{even } j} |u_j^{n+1} - u_{j-1}^{n+1}| + |u_{j-1}^{n+1} - u_{j-2}^{n+1}|\\
&= \sum_{\text{even } j} \Big|(1-\lambda)^2\left(u_j^n - u_{j-1}^n\right) + 2\lambda(1-\lambda)\\
&\quad \times \left(u_{j-2}^n - u_{j-3}^n\right) + \lambda\left(u_{j-3}^n - u_{j-4}^n\right)\\
&\quad + \lambda^2\left(u_{j-4}^n - u_{j-5}^n\right)\Big| + \Big|(1-\lambda)\left(u_{j-1}^n - u_{j-2}^n\right)\Big|.\\
&\le \sum_{\text{even } j} (1-\lambda)^2|u_j^n - u_{j-1}^n| + (1-\lambda)^2|u_{j-1}^n - u_{j-2}^n|\\
&\quad + \lambda(1-\lambda)|u_{j-1}^n - u_{j-2}^n| + 2\lambda(1-\lambda)|u_{j-2}^n - u_{j-3}^n|\\
&\quad + \lambda|u_{j-3}^n - u_{j-4}^n| + \lambda^2|u_{j-4}^n - u_{j-5}^n|\\
&= (1-\lambda)^2\,\mathrm{TV}(u^n) + \sum_{\text{even } j} \lambda(1-\lambda)|u_{j-1}^n - u_{j-2}^n|\\
&\quad + \lambda(1-\lambda)|u_{j-2}^n - u_{j-3}^n| + \lambda(1-\lambda)|u_{j-2}^n - u_{j-3}^n|\\
&\quad + \lambda|u_{j-3}^n - u_{j-4}^n| + \lambda^2|u_{j-4}^n - u_{j-5}^n|\\
&= ((1-\lambda)^2 + \lambda(1-\lambda))\,\mathrm{TV}(u^n)\\
&\quad + \sum_{\text{even } j} \lambda(1-\lambda)|u_{j-2}^n - u_{j-3}^n|\\
&\quad + \lambda(1-\lambda)|u_{j-3}^n - u_{j-4}^n|\\
&\quad + (\lambda - \lambda(1-\lambda))|u_{j-3}^n - u_{j-4}^n| + \lambda^2|u_{j-4}^n - u_{j-5}^n|\\
&= ((1-\lambda)^2 + 2\lambda(1-\lambda))\,\mathrm{TV}(u^n)\\
&\quad + \sum_{\text{even } j} \lambda^2|u_{j-3}^n - u_{j-4}^n| + \lambda^2|u_{j-4}^n - u_{j-5}^n|\\
&= ((1-\lambda)^2 + 2\lambda(1-\lambda) + \lambda^2)\,\mathrm{TV}(u^n)\\
&= \mathrm{TV}(u^n)
\end{aligned}$$

Similarly, for the additive scheme, we have

$$\begin{aligned}
&\mathrm{TV}(u^{n+1})\\
&= \sum_{\text{even } j} |u_j^{n+1} - u_{j-1}^{n+1}| + |u_{j-1}^{n+1} - u_{j-2}^{n+1}|\\
&= \sum_{\text{even } j} \Big|(1-\lambda)\left(u_j^n - u_{j-1}^n\right) + \lambda\left(u_{j-2}^n - u_{j-3}^n\right)\\
&\quad + \lambda\left(u_{j-3}^n - u_{j-4}^n\right)\Big| + \Big|(1-\lambda)\left(u_{j-1}^n - u_{j-2}^n\right)\Big|\\
&\le \sum_{\text{even } j} (1-\lambda)|u_j^n - u_{j-1}^n| + (1-\lambda)|u_{j-1}^n - u_{j-2}^n|\\
&\quad + \lambda|u_{j-2}^n - u_{j-3}^n| + \lambda|u_{j-3}^n - u_{j-4}^n|\\
&= \mathrm{TV}(u^n).
\end{aligned}$$

□

For the multilevel algorithms, it turns out that the multiplicative algorithm does not preserve monotonicity in general. However, the oscillations appear to be very small and do not seem to affect the fast wave propagation; see the numerical results in Sect. 6. For the multilevel additive scheme, it still has the monotonicity preserving and TVD properties. We first extend the formulae in (10) and (11) to the multilevel case.

Lemma 4.1 *For the k-level additive multigrid time stepping scheme, and $j = 2^{k-1}$, it holds that*

$$u_j^{n+1} - u_{j-1}^{n+1} = (1-\lambda)\left(u_j^n - u_{j-1}^n\right) + \lambda\left(u_{j-2^{k-1}}^n - u_{j-2^k}^n\right)$$
$$u_{j-m}^{n+1} - u_{j-m-1}^{n+1} = (1-\lambda)\left(u_{j-m}^n - u_{j-m-1}^n\right)$$

$m = 1, \ldots, 2^{k-1} - 1.$

Proof We prove by induction. Suppose L is the number of multigrid levels. For $L = 2$, it is proved in the proof of Theorem 4.1. Suppose it is true for $L = k$, and consider the case $L = k+1$. For j=a constant multiple of 2^{k+1},

$$u_j^{n+1} = \tilde{u}_j^{(2)}$$
$$u_{j-1}^{n+1} = \bar{u}_{j-1}^{(1)} + \tilde{u}_{j-2}^{(2)} - u_{j-2}^n,$$

where the superscript (1) denotes functions on the first grid, which is also the finest grid, and (2) functions on the second grid. Subtracting the two,

$$u_j^{n+1} - u_{j-1}^{n+1} = \tilde{u}_j^{(2)} - \tilde{u}_{j-2}^{(2)} - (1-\lambda)\left(u_{j-1}^n - u_{j-2}^n\right).$$

Since we use the previous values u^n on all the coarse grids, the update of $\tilde{u}_j^{(2)}$ from $u_j^{(2)}$, $j = 0, 2, \ldots$, is completely independent of the update on the finest grid. In other words, $\tilde{u}_j^{(2)}$ can be thought of being obtained by applying the level k additive scheme to u^n on the even points. By induction hypothesis, we have

$$\begin{aligned} u_j^{n+1} - u_{j-1}^{n+1} &= (1-\lambda)\left(u_j^n - u_{j-2}^n\right) + \lambda\left(u_{j-2^k}^n - u_{j-2^{k+1}}^n\right) \\ &\quad - (1-\lambda)\left(u_{j-1}^n - u_{j-2}^n\right) \\ &= (1-\lambda)\left(u_j^n - u_{j-1}^n\right) + \lambda\left(u_{j-2^k}^n - u_{j-2^{k+1}}^n\right). \end{aligned}$$

Similarly, since $u_{j-2}^{n+1} = \tilde{u}_{j-2}^{(2)}$, we have

$$\begin{aligned} u_{j-1}^{n+1} - u_{j-2}^{n+1} &= \bar{u}_{j-1} + \tilde{u}_{j-2}^{(2)} - u_{j-2}^n - \tilde{u}_{j-2}^{(2)} \\ &= (1-\lambda)\left(u_{j-1}^n - u_{j-2}^n\right). \end{aligned}$$

We compute one more difference:

$$\begin{aligned} u_{j-2}^{n+1} - u_{j-3}^{n+1} &= \tilde{u}_{j-2}^{(2)} - \left(\bar{u}_{j-3}^{(1)} - \tilde{u}_{j-4}^{(2)} - u_{j-4}^n\right) \\ &= (1-\lambda)\left(u_{j-2}^n - u_{j-3}^n\right), \end{aligned}$$

by induction hypothesis on $\tilde{u}_{j-2}^{(2)} - \tilde{u}_{j-4}^{(2)}$. The rest is essentially the same and we shall omit the calculations. In conclusion, the formulae are also true for $L = k+1$. □

Theorem 4.3 *The multilevel additive multigrid time stepping scheme preserves monotonicity and are TVD.*

Proof The monotonicity preserving property is clear from the formulae given by Lemma 4.1. The TVD property can be seen by (assuming k-level)

$$\begin{aligned} &\mathrm{TV}(u^{n+1}) \\ &\quad = \sum_j \left|u_j^{n+1} - u_{j-1}^{n+1}\right| \\ &\quad = \sum_{j=\text{multiple of } 2^{k-1}} \Big(\left|u_j^{n+1} - u_{j-1}^{n+1}\right| + \left|u_{j-1}^{n+1} - u_{j-2}^{n+1}\right| \\ &\qquad + \cdots + \left|u_{j-2^{k-1}+1}^{n+1} - u_{j-2^{k-1}}^{n+1}\right|\Big) \\ &\quad = \sum_{j=\text{multiple of } 2^{k-1}} \Big[\Big|(1-\lambda)\left(u_j^n - u_{j-1}^n\right) \\ &\qquad + \lambda\left(u_{j-2^{k-1}}^n - u_{j-2^k}^n\right)\Big| + (1-\lambda)\left|u_{j-1}^n - u_{j-2}^n\right| \\ &\qquad + \cdots + (1-\lambda)\left|u_{j-2^{k-1}+1}^n - u_{j-2^{k-1}}^n\right|\Big] \\ &\quad \le (1-\lambda)\mathrm{TV}(u^n) + \lambda\mathrm{TV}(u^n) \\ &\quad = \mathrm{TV}(u^n). \end{aligned}$$

□

4.1 Convergence analysis

In this section, we analyze the convergence property of the two-level multiplicative scheme by means of Fourier analysis. Our results show that waves of *both* low and high frequency propagate with the speed of 4, in contrast with the Fourier analysis given by Gustafsson and Lötstedt which showed that, for their multigrid method, the smooth low frequency waves propagate with speed 3. This is expected since the linear two-level schemes have been proven to be nonoscillatory and hence should not have any dispersive effect.

Consider the update formula (6) for u^{n+1}. We can express it in terms of matrices instead of the interpolation operator $\mathcal{P}$:

$$\begin{aligned} u^{n+1} &= \bar{u}^h + P_{\text{odd}}\left(\bar{u}^H - R_u u^n\right) \\ &\quad + P_{\text{even}}\left(\bar{u}^H - R_u \bar{u}^h\right), \end{aligned} \tag{12}$$

where

$$P_{\text{odd}} = \begin{bmatrix} 0 & & \\ 1 & & \\ & 0 & \\ & 1 & \\ & & \ddots \end{bmatrix}, P_{\text{even}} = \begin{bmatrix} 1 & & \\ 0 & & \\ & 1 & \\ & 0 & \\ & & \ddots \end{bmatrix}, R_u = P_{\text{even}}^T.$$

Noting that $\bar{u}^h = (I - \lambda A^h)u^n$ and $\bar{u}^H = (I - \lambda A^H)R_u u^n$, (12) can be written as $u^{n+1} = Mu^n$, where the iteration matrix M is given by

$$\begin{aligned} M &= [I + P_{\text{odd}}R_u - \lambda(P_{\text{even}} + P_{\text{odd}})A^H R_u](I - \lambda A^h) \\ &\quad - P_{\text{odd}}R_u. \end{aligned}$$

Following the standard Fourier analysis for multigrid methods, let

$$\mathrm{e}^{\mu}(x_j) = \mathrm{e}^{i\mu\pi x_j} \quad -N+1 \le \mu \le N,$$

be the Fourier basis of frequency μ. The Fourier transform matrix has e^{μ}'s as columns, and each low frequency

μ, $-N/2+1 \le \mu \le N/2$, is paired with the corresponding high frequency $\mu' = \mu + N$. Under this ordering, it is well-known that the Fourier transformed iteration matrix, $\hat{M}$, is block diagonal:

$$\hat{M} = \text{blkdiag}(\hat{M}_1, \ldots, \hat{M}_{N/2}),$$

where each $\hat{M}_\mu$ is a 2×2 matrix. By examining $\hat{M}_\mu$, we can determine the convergence and propagation properties of u^n. We first state the Fourier transform result.

Lemma 4.2 *The Fourier transformed iteration matrix is given by*

$$\hat{M}_\mu = [I + (\hat{P}_{\text{odd}})_\mu (\hat{R}_u)_\mu - \lambda((\hat{P}_{\text{odd}})_\mu + (\hat{P}_{\text{even}})_\mu) \hat{A}^H_\mu (\hat{R}_u)_\mu](I - \lambda \hat{A}^h_\mu) - (\hat{P}_{\text{odd}})_\mu (\hat{R}_u)_\mu,$$

where

$$\hat{A}^h_\mu = \begin{bmatrix} 1 - \mathrm{e}^{-\mu\pi hi} & 0 \\ 0 & 1 + \mathrm{e}^{-\mu\pi hi} \end{bmatrix}, \qquad \hat{A}^H_\mu = 1 - \mathrm{e}^{-2\mu\pi hi}$$

$$(\hat{P}_{\text{odd}})_\mu = \frac{1}{\sqrt{2}} \begin{bmatrix} \mathrm{e}^{-\mu\pi hi} \\ -\mathrm{e}^{-\mu\pi hi} \end{bmatrix}, \qquad (\hat{P}_{\text{even}})_\mu = \frac{1}{\sqrt{2}} \begin{bmatrix} 1 \\ 1 \end{bmatrix},$$

$$(\hat{R}_u)_\mu = (\hat{P}_{\text{even}})^T_\mu.$$

Theorem 4.4 *For* $\lambda = 1.0$, *the speed of wave propagation of any frequency is* 4.

Proof Simplifying the formula for $\hat{M}_\mu$ in Lemma 4.2 with $\lambda = 1.0$, we obtain

$$\hat{M}_\mu = \mathrm{e}^{-3.5\mu\pi hi} \begin{bmatrix} \cos(\mu\pi h/2) & -\cos(\mu\pi h/2) \\ i\sin(\mu\pi h/2) & -i\sin(\mu\pi h/2) \end{bmatrix}.$$

The eigenvalues of $\hat{M}_\mu$ are 0 and $\mathrm{e}^{-4\mu\pi hi}$, and hence the wave propagates with the speed of 4, independent of the frequency. □

We remark that there is no damping for $\lambda = 1.0$ since the upwind smoothing is exact. In general, for $\lambda < 1.0$, it can be proved that the high frequencies are damped out. Nevertheless, the key of this approach is to expell the error out of the boundary via rapid propagation on multiple grids; the effect of damping is not as important as in elliptic multigrid methods.

5 Nonlinear analysis

We analyze the monotonicity preserving property of the nonlinear multigrid time stepping schemes proposed in Sect. 3.2 for solving the scalar conservation laws (6) where the flux function is assumed to be convex. We shall show that the interpolation operator derived from the local Riemann solutions will lead to a nonoscillatory multigrid time stepping scheme. Since the analysis for the nonlinear case is much harder, we only consider the two-level additive scheme. The effectiveness of the multilevel multiplicative and additive schemes are demonstrated empirically in Sect. 6.

Although the proposed nonlinear multigrid time stepping schemes allow essentially any monotonicity preserving schemes as smoothers, in the analysis, we focus on the EO scheme since the nonlinear switching via the maximum and minimum functions can be replaced by integrals.

Lemma 5.1 ([8]) *The EO smoothing scheme can be written as*

$$u_j^{n+1} = u_j^n - \lambda \int_{u_j^n}^{u_{j+1}^n} f'\chi \,\mathrm{d}s - \lambda \int_{u_{j-1}^n}^{u_j^n} f'(1-\chi)\,\mathrm{d}s,$$

where $\chi(u)$ *is defined as*

$$\chi(u) = \begin{cases} 0 \text{ if } f'(u) \ge 0 \\ 1 \text{ if } f'(u) < 0. \end{cases}$$

Moreover, we have the following inequalities:

$$\begin{aligned} -f'(u)\chi(u) &\ge 0 \\ 1 + \lambda f'(u)(2\chi(u) - 1) &\ge 0 \\ f'(u)(1 - \chi(u)) &\ge 0 \end{aligned}$$

provided the CFL condition is satisfied: $\left|\lambda f'(u)\right| \le 1$.

We consider the interval (x_{j-2}, x_j), j = even, and compute $u_j^{n+1} - u_{j-1}^{n+1}$ and $u_{j-1}^{n+1} - u_{j-2}^{n+1}$, where u^{n+1} is obtained from the two-level nonlinear additive multigrid time stepping scheme. Since our interpolation is defined by the local Riemann solution which depends on the signs of $f'(u_{j-2}^n)$, $f'(u_{j-1}^n)$, and $f'(u_j^n)$, we separate the computations into four cases, each of which is presented as a lemma.

Lemma 5.2 *Suppose* $f'(u_{j-2}^n) \ge 0$ *and* $f'(u_j^n) \ge 0$. *If* u^n *is monotonically nondecreasing* (*nonincreasing*), *so is* u^{n+1}.

Proof We assume that u^n is monotonically nondecreasing; the other case can be handled similarly. Since u^n is monotone and the flux $f(u)$ is convex, it implies that $f'(u_{j-1}^n) \ge 0$. Thus, our Riemann solution interpolation gives

$$u_{j-1}^{n+1} = \bar{u}_{j-1}^{(1)} + \bar{u}_{j-2}^{(2)} - u_{j-2}^{n}.$$

In the coarse grid evolution, in general, we also have the forcing term due to the residual on the fine grid:

$$\bar{u}_{j-2}^{(2)} = u_{j-1}^{n} - \lambda \int_{u_{j-2}^{n}}^{u_{j}^{n}} f'\chi \, \mathrm{d}s - \lambda \int_{u_{j-4}^{n}}^{u_{j-2}^{n}} f'(1-\chi)\, \mathrm{d}s + \Delta t^{(2)}\, b_{j-2}^{(2)},$$

where the forcing term is defined as

$$b_{j-2}^{(2)} \equiv \frac{1}{\Delta x^{(2)}} \left(\int_{u_{j-2}^{n}}^{u_{j}^{n}} f'\chi \, \mathrm{d}s + \int_{u_{j-4}^{n}}^{u_{j-2}^{n}} f'(1-\chi)\, \mathrm{d}s \right) - \mathcal{R}_{nl}(\bar{r}^{(1)})_{j-2}.$$

Our nonlinear Riemann solution restriction gives

$$\begin{aligned}
b_{j-2}^{(2)} &= \frac{1}{\Delta x^{(2)}} \left(\int_{u_{j-2}^{n}}^{u_{j}^{n}} f'\chi \, \mathrm{d}s + \int_{u_{j-4}^{n}}^{u_{j-2}^{n}} f'(1-\chi)\, \mathrm{d}s \right) - \frac{1}{2}(\bar{r}_{j-2}^{(1)} + \bar{r}_{j-3}^{(1)}) \\
&= \frac{1}{\Delta x^{(2)}} \left(\int_{u_{j-2}^{n}}^{u_{j}^{n}} f'\chi \, \mathrm{d}s + \int_{u_{j-4}^{n}}^{u_{j-2}^{n}} f'(1-\chi)\, \mathrm{d}s \right) \\
&\quad - \frac{1}{2}\frac{1}{\Delta x^{(1)}} \left(\int_{u_{j-2}^{n}}^{u_{j-1}^{n}} f'\chi \, \mathrm{d}s + \int_{u_{j-3}^{n}}^{u_{j-2}^{n}} f'(1-\chi)\, \mathrm{d}s + \int_{u_{j-3}^{n}}^{u_{j-2}^{n}} f'\chi \, \mathrm{d}s + \int_{u_{j-4}^{n}}^{u_{j-3}^{n}} f'(1-\chi)\, \mathrm{d}s \right) \\
&= \frac{1}{\Delta x^{(2)}} \left(\int_{u_{j-3}^{n}}^{u_{j-2}^{n}} f'\chi \, \mathrm{d}s + \int_{u_{j-1}^{n}}^{u_{j}^{n}} f'\chi \, \mathrm{d}s \right) \\
&= \frac{1}{\Delta x^{(2)}} \int_{u_{j-3}^{n}}^{u_{j-2}^{n}} f'\chi \, \mathrm{d}s,
\end{aligned}$$

since $\int_{u_{j-1}^{n}}^{u_{j}^{n}} f'\chi \, \mathrm{d}s = 0$ on the interval (u_{j-1}^{n}, u_{j}^{n}). Hence

$$\begin{aligned}
u_{j}^{n+1} - u_{j-1}^{n+1} &= \bar{u}_{j}^{(2)} - \bar{u}_{j-1}^{(1)} - \bar{u}_{j-2}^{(2)} + u_{j-2}^{n} \\
&= u_{j}^{n} - \lambda \int_{u_{j}^{n}}^{u_{j+2}^{n}} f'\chi \, \mathrm{d}s - \lambda \int_{u_{j-2}^{n}}^{u_{j}^{n}} f'(1-\chi)\, \mathrm{d}s - u_{j-1}^{n} \\
&\quad + \lambda \int_{u_{j-1}^{n}}^{u_{j}^{n}} f'\chi \, \mathrm{d}s + \lambda \int_{u_{j-2}^{n}}^{u_{j-1}^{n}} f'(1-\chi)\, \mathrm{d}s - u_{j-2}^{n} \\
&\quad + \lambda \int_{u_{j-2}^{n}}^{u_{j}^{n}} f'\chi \, \mathrm{d}s + \lambda \int_{u_{j-4}^{n}}^{u_{j-2}^{n}} f'(1-\chi)\, \mathrm{d}s \\
&\quad - \lambda \int_{u_{j-3}^{n}}^{u_{j-2}^{n}} f'\chi \, \mathrm{d}s + u_{j-2}^{n} \\
&= u_{j}^{n} - u_{j-1}^{n} - \lambda \int_{u_{j}^{n}}^{u_{j+2}^{n}} f'\chi \, \mathrm{d}s + \lambda \int_{u_{j-2}^{n}}^{u_{j}^{n}} f'(2\chi - 1)\, \mathrm{d}s \\
&\quad + \lambda \int_{u_{j-1}^{n}}^{u_{j}^{n}} f'\chi \, \mathrm{d}s + \lambda \int_{u_{j-2}^{n}}^{u_{j-1}^{n}} f'(1-\chi)\, \mathrm{d}s \\
&\quad + \lambda \int_{u_{j-4}^{n}}^{u_{j-2}^{n}} f'(1-\chi)\, \mathrm{d}s - \lambda \int_{u_{j-3}^{n}}^{u_{j-2}^{n}} f'\chi \, \mathrm{d}s \\
&= \int_{u_{j-1}^{n}}^{u_{j}^{n}} 1 + \lambda f'(2\chi - 1)\, \mathrm{d}s + \lambda \int_{u_{j-2}^{n}}^{u_{j}^{n}} f'\chi \, \mathrm{d}s \\
&\quad - \lambda \int_{u_{j}^{n}}^{u_{j+2}^{n}} f'\chi \, \mathrm{d}s - \lambda \int_{u_{j-3}^{n}}^{u_{j-2}^{n}} f'\chi \, \mathrm{d}s \\
&\quad + \lambda \int_{u_{j-4}^{n}}^{u_{j-2}^{n}} f'(1-\chi)\, \mathrm{d}s.
\end{aligned}$$

Since $f'(u) \geq 0$ for $u_{j-2}^{n} \leq u \leq u_{j}^{n}$, $\chi(u) = 0$, and hence $\int_{u_{j-2}^{n}}^{u_{j}^{n}} f'\chi \, \mathrm{d}s = 0$. By Lemma 5.1, all the integrands on the right-hand side are nonnegative, and therefore

$u_j^{n+1} - u_{j-1}^{n+1} \geq 0$. Similarly,

$$
\begin{aligned}
&u_{j-1}^{n+1} - u_{j-2}^{n+1} \\
&= \bar{u}_{j-1}^n + \bar{u}_{j-2}^{(2)} - u_{j-2}^n - \bar{u}_{j-2}^{(2)} \\
&= u_{j-1}^n - \lambda \int_{u_{j-1}^n}^{u_j^n} f'\chi \, \mathrm{d}s - \lambda \int_{u_{j-2}^n}^{u_{j-1}^n} f'(1-\chi)\, \mathrm{d}s - u_{j-2}^n \\
&= \int_{u_{j-2}^n}^{u_{j-1}^n} 1 - \lambda f'(1-\chi)\, \mathrm{d}s - \lambda \int_{u_{j-1}^n}^{u_j^n} f'\chi \, \mathrm{d}s \\
&\geq 0,
\end{aligned}
$$

by Lemma 5.1 and the CFL condition: $|\lambda f'(u)| \leq 1$. □

Lemma 5.3 *Suppose $f'(u_{j-2}^n) \leq 0$ and $f'(u_j^n) \leq 0$. If u^n is monotonically nondecreasing (nonincreasing), so is u^{n+1}.*

Proof Similar to the proof in Lemma 5.2. □

Lemma 5.4 *Suppose $f'(u_{j-2}^n) < 0$ and $f'(u_j^n) > 0$. If u^n is monotonically nondecreasing, so is u^{n+1}.*

Proof (Note that since f is convex and u^n is monotone, u^n cannot be decreasing.) This is the case of transonic rarefaction. The Riemann solution interpolation gives $u_{j-1}^{n+1} = \bar{u}_{j-1}^{(1)}$. Moreover, $b_j^{(2)} = 0$. If $f'(u_{j-1}^n) \geq 0$, then

$$
\begin{aligned}
b_j^{(2)} &= \frac{1}{\Delta x^{(2)}} \left(\int_{u_j^n}^{u_{j+2}^n} f'\chi \, \mathrm{d}s + \int_{u_{j-2}^n}^{u_j^n} f'(1-\chi)\, \mathrm{d}s \right) \\
&\quad - \frac{1}{2}(\bar{r}_{j-1}^{(1)} + \bar{r}_j^{(1)}) \\
&= \frac{1}{\Delta x^{(2)}} \left(\int_{u_{j+1}^n}^{u_{j+2}^n} f'\chi \, \mathrm{d}s - \int_{u_{j-1}^n}^{u_j^n} f'\chi \, \mathrm{d}s \right) \\
&= 0,
\end{aligned}
$$

since $f'(u) \geq 0$ for $u \geq u_{j-1}^n$. If $f'(u_{j-1}^n) < 0$, then

$$
\begin{aligned}
b_j^{(2)} &\equiv \frac{1}{\Delta x^{(2)}} \left(\int_{u_j^n}^{u_{j+2}^n} f'\chi \, \mathrm{d}s + \int_{u_{j-2}^n}^{u_j^n} f'(1-\chi)\, \mathrm{d}s \right) - \frac{1}{2}\bar{r}_j^{(1)} \\
&= \frac{1}{\Delta x^{(2)}} \left(\int_{u_{j+1}^n}^{u_{j+2}^n} f'\chi \, \mathrm{d}s + \int_{u_{j-2}^n}^{u_{j-1}^n} f'(1-\chi)\, \mathrm{d}s \right) = 0.
\end{aligned}
$$

By similar computations, we can also show that $b_{j-2}^{(2)} = 0$. Hence,

$$
\begin{aligned}
&u_j^{n+1} - u_{j-1}^{n+1} \\
&= \bar{u}_j^{(2)} - \bar{u}_{j-1}^{(1)} \\
&= u_j^n - \lambda \int_{u_j^n}^{u_{j+2}^n} f'\chi \, \mathrm{d}s - \lambda \int_{u_{j-2}^n}^{u_j^n} f'(1-\chi)\, \mathrm{d}s - u_{j-1}^n \\
&\quad + \lambda \int_{u_{j-1}^n}^{u_j^n} f'\chi \, \mathrm{d}s + \lambda \int_{u_{j-2}^n}^{u_{j-1}^n} f'(1-\chi)\, \mathrm{d}s \\
&= \int_{u_{j-1}^n}^{u_j^n} 1 + \lambda f'(2\chi - 1)\, \mathrm{d}s - \lambda \int_{u_j^n}^{u_{j+2}^n} f'\chi \, \mathrm{d}s \\
&\geq 0,
\end{aligned}
$$

by Lemma 5.1. Similarly,

$$
\begin{aligned}
&u_{j-1}^{n+1} - u_{j-2}^{n+1} \\
&= \bar{u}_{j-1}^{(1)} - \bar{u}_{j-2}^{(2)} \\
&= u_{j-1}^n - \lambda \int_{u_{j-1}^n}^{u_j^n} f'\chi \, \mathrm{d}s - \lambda \int_{u_{j-2}^n}^{u_{j-1}^n} f'(1-\chi)\, \mathrm{d}s - u_{j-2}^n \\
&\quad + \lambda \int_{u_{j-2}^n}^{u_j^n} f'\chi \, \mathrm{d}s + \lambda \int_{u_{j-4}^n}^{u_{j-2}^n} f'(1-\chi)\, \mathrm{d}s \\
&= \int_{u_{j-2}^n}^{u_{j-1}^n} 1 + \lambda f'(2\chi - 1)\, \mathrm{d}s + \lambda \int_{u_{j-4}^n}^{u_{j-2}^n} f'(1-\chi)\, \mathrm{d}s \\
&\quad \geq 0.
\end{aligned}
$$

□

Lemma 5.5 *Suppose $f'(u_{j-2}^n) \geq 0$ and $f'(u_j^n) \leq 0$. If u^n is monotonically nonincreasing, so is u^{n+1}.*

Proof This is the case of a shock. As opposed to the rarefaction case, u^n cannot be increasing. Assume first that $f'(u_{j-1}^n) \geq 0$. Then our interpolation gives

$$
u_{j-1}^{n+1} = \bar{u}_{j-1}^{(1)} + \bar{u}_{j-2}^{(2)} - u_{j-2}^n.
$$

In this case, $b_{j-2}^{(2)}=0$ since $f'(u_{j-3}^n), f'(u_{j-2}^n), f'(u_{j-1}^n) \geq 0$ (cf. Lemma 5.2). However, $b_j^{(2)} \neq 0$, and it can be shown that

$$
\begin{aligned}
b_j^{(2)} &\equiv \frac{1}{2h}\left(\int_{u_j^n}^{u_{j+2}^n} f'\chi \, ds + \int_{u_{j-2}^n}^{u_j^n} f'(1-\chi)\, ds\right) \\
&\quad - \frac{1}{2}(\bar{r}_{j-1}^{(1)} + \bar{r}_j^{(1)} + \bar{r}_{j+1}^{(1)}) \\
&= \frac{-1}{2h}\left(\int_{u_{j-1}^n}^{u_j^n} f'\chi \, ds + \int_{u_j^n}^{u_{j+1}^n} f'(1-\chi)\, ds\right) \\
&= \frac{-1}{2h}\int_{u_{j-1}^n}^{u_j^n} f'\chi \, ds,
\end{aligned}
$$

since $f'(u_j^n), f'(u_{j+1}^n) \leq 0$. Thus $\bar{u}_j^{(2)}$ becomes

$$
\begin{aligned}
\bar{u}_j^{(2)} &= u_j^n - \lambda \int_{u_j^n}^{u_{j+2}^n} f'\chi \, ds - \lambda \int_{u_{j-2}^n}^{u_j^n} f'(1-\chi)\, ds \\
&\quad - \lambda \int_{u_{j-1}}^{u_j^n} f'\chi \, ds.
\end{aligned}
$$

Combining all these formulae, we have

$$
\begin{aligned}
&u_j^{n+1} - u_{j-1}^{n+1} \\
&\quad = \bar{u}_j^{(2)} - \bar{u}_{j-1}^{(1)} - \bar{u}_{j-2}^{(2)} + u_{j-2}^n \\
&\quad = \int_{u_{j-1}^n}^{u_j^n} 1 + \lambda f'(2\chi - 1)\, ds + \lambda \int_{u_{j-2}^n}^{u_{j-1}^n} f'\chi \, ds \\
&\qquad - \lambda \int_{u_j^n}^{u_{j+2}^n} f'\chi \, ds + \lambda \int_{u_{j-4}^n}^{u_{j-2}^n} f'(1-\chi)\, ds \\
&\quad \leq 0,
\end{aligned}
$$

since $\lambda \int_{u_{j-2}^n}^{u_{j-1}^n} f'\chi \; ds = 0$ because $f'(u_{j-2}^n), f'(u_{j-1}^n) \geq 0$, and the remaining terms are all nonpositive by Lemma 5.1 and the fact that u^n is nonincreasing. Similarly,

$$
\begin{aligned}
u_{j-1}^{n+1} - u_{j-2}^{n+1} &= \bar{u}_{j-1}^{(1)} + \bar{u}_{j-1}^{(2)} - u_{j-2}^n - \bar{u}_{j-2}^{(1)} \\
&= \int_{u_{j-1}^n}^{u_{j-2}^n} 1 - \lambda f'(1-\chi)\, ds - \lambda \int_{u_{j-1}^n}^{u_j^n} f'\chi \, ds \\
&\leq 0.
\end{aligned}
$$

The case where $f'(u_{j-1}^n) < 0$ is analogous and it will be omitted here. □

Theorem 5.1 *The two-level additive multigrid time stepping scheme preserves monotonicity.*

Proof In the convex case, the four possible cases of $f'(u_{j-2}^n)$ and $f'(u_j^n)$ are proved in Lemma 5.2-5.5, and hence the result. □

6 Numerical results

In this section, we verify numerically that the linear and nonlinear multigrid time stepping schemes are nonoscillatory and the steady state solution can be reached in small number of multigrid cycles. We consider the linear wave equation (1) and the nonlinear Burgers' equation:

$$u_t + \left(\frac{1}{2}u^2\right)_x = 0 \quad 0 < x < 1,$$

with appropriate boundary and initial conditions.

For the linear wave equation, the boundary condition is chosen as 0 and the initial condition is a square wave. Therefore, the steady state solution $u \equiv 0$. We apply the 3-level multiplicative and additive schemes to solving the equation with CFL number $\lambda = 1.0$. Thus, the smoothing step given by the upwinding is in fact exact evolution. The results are shown in Figs. 8 and 9,

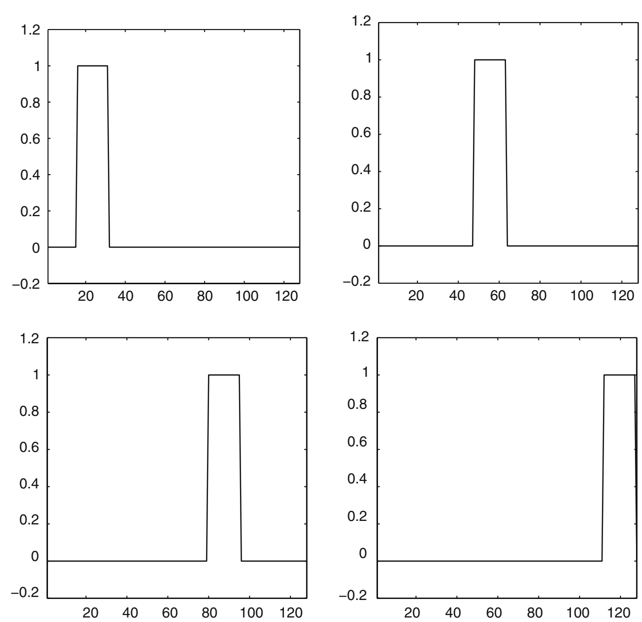

Fig. 8 The numerical solution given by the 3-level multiplicative scheme, $\lambda = 1.0$, at (*top-left*) time step = 0, (*top-right*) time step = 4, (*bottom-left*) time step = 8, (*bottom-right*) time step = 12

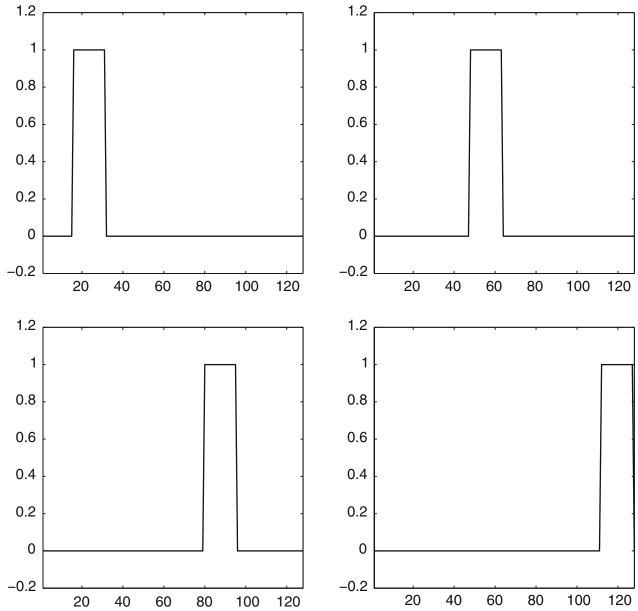

Fig. 9 The numerical solution given by the 3-level additive scheme, $\lambda = 1.0$, at (*top-left*) time step $= 0$, (*top-right*) time step $= 8$, (*bottom-left*) time step $= 16$, (*bottom-right*) time step $= 24$.

respectively. First, contrast with the standard multigrid approach (see Fig. 1), the initial square wave remains as a square wave as it propagates. We remark that the multiplicative scheme in general does not preserve monotonicity and is not TVD when the number of grids is more than 2, but with the special choice of CFL number, $\lambda = 1.0$, no oscillations occurred.

Secondly, the theoretically results by Jespersen [19] and Gustafsson and Lötstedt [12] estimate that the optimal speed of propagation is:

$$\text{optimal speed of multigrid} = 2^k - 1,$$

where k is the number of grids. Our convergence result in Sect. 4.1, however, suggests a speed up of 2^k. By careful inspection, we can see that the speed of propagation of the wave given by the multiplicative scheme is indeed $2^3 = 8$ times faster than the speed of upwinding on a single grid, since the wave takes $128/8 \approx 16$ multigrid cycles to propagate out of the boundary. Thus, it achieves the theoretical optimal speed while the oscillations produced by the standard multigrid method delay the convergence.

Comparing the propagation speeds of the multiplicative and the additive schemes (Figs. 8 and 9), the former is twice as fast as the latter (cf Gauss-Seidel vs. Jacobi).

When the CFL number $\neq 1.0$, e.g. $\lambda = 0.5$, the upwind smoothing is dissipative. Moreover, the multiplicative scheme introduces oscillations. In Fig. 10, second left plot, we can see a small dip on the top of the solution; i.e. the scheme does not preserve monotonicity and is not TVD. However, we note that the oscillations appear to be very minimal and do not seem to affect the fast wave propagation. The additive scheme remains nonoscillatory, as is proved in Sect. 4; see Fig. 11.

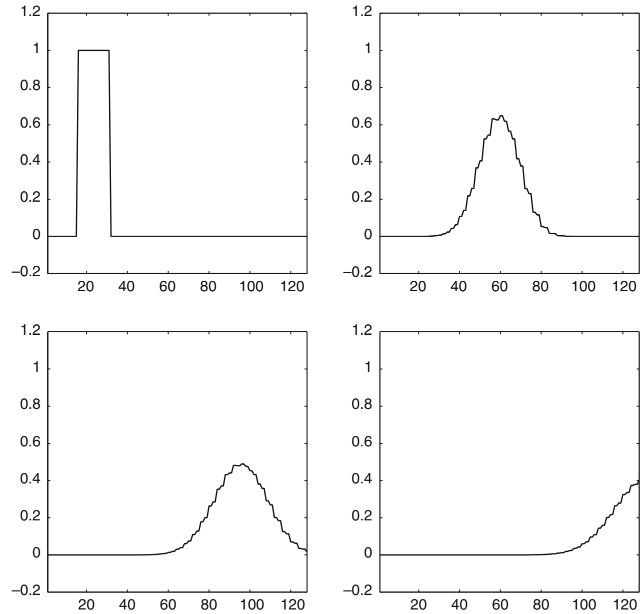

Fig. 10 The numerical solution given by the 3-level multiplicative scheme, $\lambda = 0.5$, at (*top-left*) time step $= 0$, (*top-right*) time step $= 8$, (*bottom-left*) time step $= 16$, (*bottom-right*) time step $= 24$

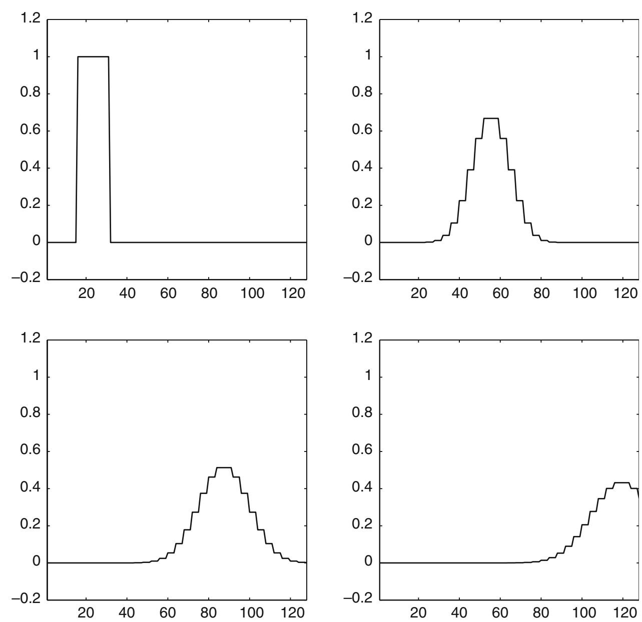

Fig. 11 The numerical solution given by the 3-level additive scheme, $\lambda = 0.5$, at (*top-left*) time step $= 0$, (*top-right*) time step $= 16$, (*bottom-left*) time step $= 32$, (*bottom-right*) time step $= 48$

Next, we apply the two schemes together with nonlinear upwind restriction and interpolation to solve the Burgers' equation. We start with a shock problem, which has also been tested by Ferm and Lötstedt [9], with boundary conditions: $u(0,t) = 1$ and $u(1,t) = -1$, and piecewise constant initial condition as shown in Figs. 12 and 13. Thus the steady state solution is

$$u = \begin{cases} 1 & \text{if } 0 \le x < 0.5 \\ -1 & \text{if } 0.5 < x \le 1. \end{cases}$$

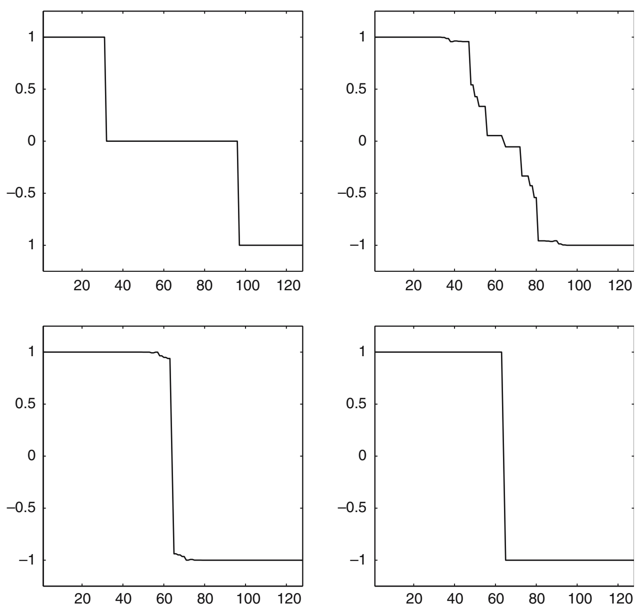

Fig. 12 The numerical solution given by the 4-level multiplicative scheme, $\lambda = 1.0$, at (*top-left*) time step = 0, (*top-right*) time step = 2, (*bottom-left*) time step = 4, (*bottom-right*) time step = 6

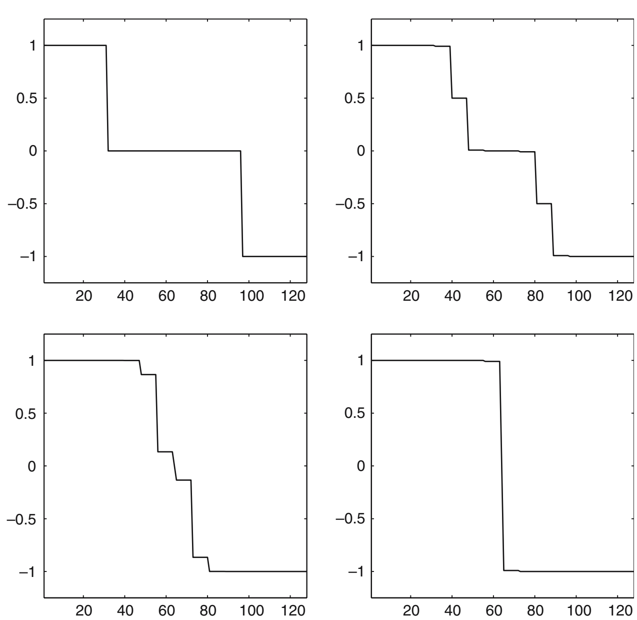

Fig. 13 The numerical solution given by the 4-level additive scheme, $\lambda = 1.0$, at (*top-left*) time step = 0, (*top-right*) time step = 3, (*bottom-left*) time step = 6, (*bottom-right*) time step = 9

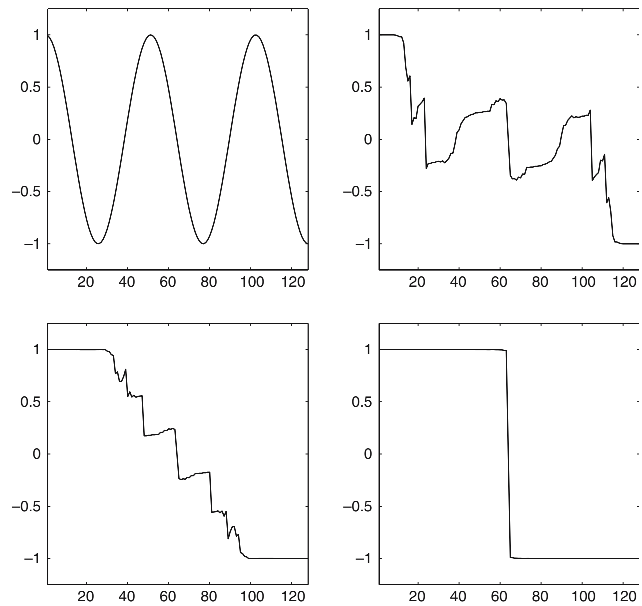

Fig. 14 The numerical solution given by the 4-level multiplicative scheme, $\lambda = 1.0$, at **a** time step = 0, **b** time step = 3, **c** time step = 6, **d** time step = 9

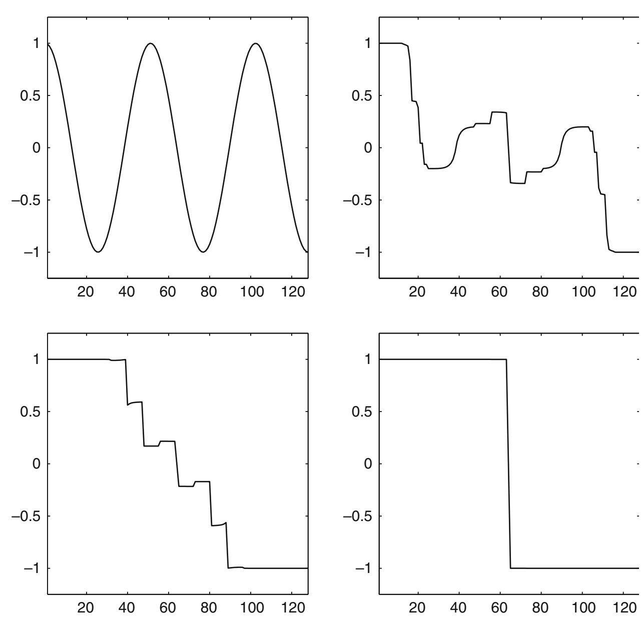

Fig. 15 The numerical solution given by the 4-level additive scheme, $\lambda = 1.0$, at (*top-left*) time step = 0, (*top-right*) time step = 6, (*bottom-left*) time step = 12, (*bottom-right*) time step = 18.

with a discontinuity at $x = 0.5$. The intermediate solutions given by the four-level multiplicative and additive schemes are shown in Figs. 12 and 13. On a single grid, EO scheme alone takes 81 time steps to reach the steady state. The optimal linear speedup for a four-level method is $2^4 = 16$, and hence the optimal number of multigrid time steps for the multiplicative scheme is $81/16 \approx 5$, which is essentially achieved by the multiplicative scheme. The four-level additive scheme takes 10 multigrid time stepping, which is about half the speedup of the multiplicative scheme, as expected.

In the previous example, only shocks are developed. We also test the schemes with the initial condition being $u(x, 0) = \cos(5\pi x)$, thus both shocks and rarefactions are developed during time steppings. The steady state solution, however, is the same as the previous example. We again apply the four-level schemes and the results are shown in Figs. 14 and 15. The single-grid EO scheme takes 143 time steps, and hence the optimal number of multigrid time steps for the multiplicative scheme is $143/16 \approx 9$. The multiplicative and additive schemes take 10 and 19 multigrid time steppings, respectively, agreeing closely with the optimal predicted values.

An extension of this approach to two dimensions is possible. However, it is noted in [17] that there exist pathological cases where multigrid with full coarsening would fail completely if the disturbances happen to lie on the noncoarse grid lines. Thus, semi-coarsening is necessary. An extension of the linear approach together with a semi-coarsening strategy is used to solve the following two-dimensional wave equation:

$$u_t + u_x + u_y = 0 \quad 0 < x,\ y < 1.$$

We use three-level and $\lambda = 0.5$. The results are shown in Fig. 16.

Finally, we present the numerical results for solving a two dimensional Burgers' equation ([31, Example 3a]):

$$u_t + \left(\frac{1}{2}u^2\right)_x + u_y = 0 \quad 0 < x, y < 1,$$

with boundary conditions: $u = -1$ on the left side, $u = 1$ on the right side, and $u = 2x - 1$ on the bottom side. Thus a shock is developed in the domain. The intermediate solutions given by the three-level multiplicative scheme, $\lambda = 0.25$, are shown in Fig. 17. On a single grid of 65×65, EO scheme takes 255 time steps to steady

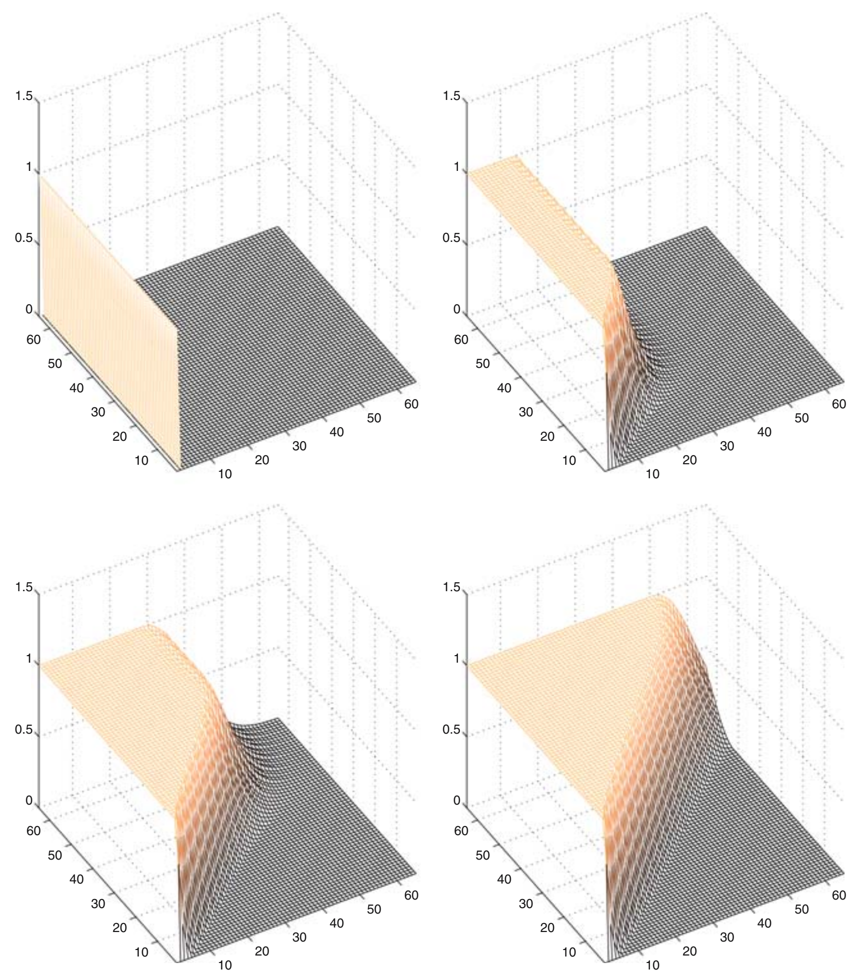

Fig. 16 The numerical solution given by the 3-level multiplicative scheme, $\lambda = 0.5$, at (*top-left*) time step = 0, (*top-right*) time step = 6, (*bottom-left*) time step = 11, (*bottom-right*) time step = 16

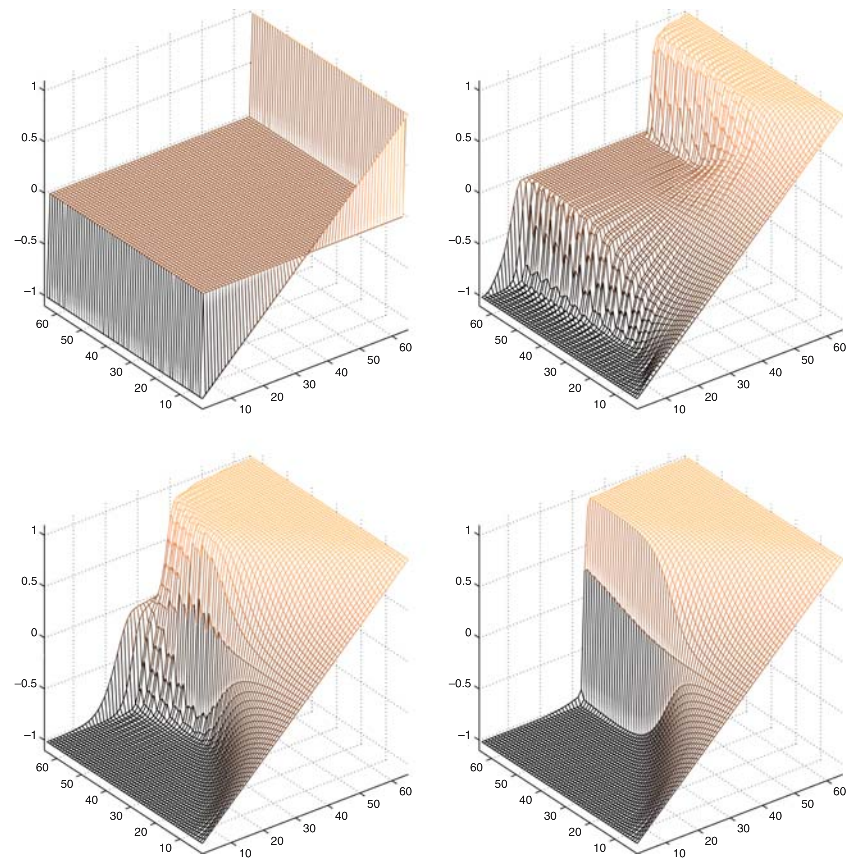

Fig. 17 The numerical solution given by the 3-level multiplicative scheme, $\lambda = 0.25$, at (*top-left*) time step = 0, (*top-right*) time step = 12, (*bottom-left*) time step = 24, (*bottom-right*) time step = 36

state. The optimal number of multigrid time steps would be $253/8 \approx 32$. The three-level method requires 36 time steps, showing similar convergence behaviour as in one-dimensional case.

7 Concluding remarks

Through the analytical and numerical results, we have demonstrated that monotonicity preserving and total variation diminishing are two key properties to obtain an efficient multigrid time stepping schemes. To achieve these properties, we have described an upwind residual restriction and interpolation which are based on the characteristics of the linear wave equation. For nonlinear conservation laws, we have proposed a nonlinear restriction and interpolation which are based on local Riemann solutions, a natural generalization of the characteristics approach.

The present study has been focused primarily on the one-dimensional case. The numerical results in two dimensions, however, have indicated the potential of this approach. Nevertheless, extensions to systems and multidimensions are yet to be investigated.

References

1. Alcouffe, R.E., Brandt, A., Dendy, J.E., Painter, J.W. Jr.: The multi-grid method for the diffusion equation with strongly discontinuous coefficients. SIAM J. Sci. Stat. Comput. **2**(4), 430–454 (1981)
2. Bramble, J.: Multigrid Methods. Longman Scientific & Technical, Essex, UK (1993)
3. Brandt, A.: Multi-level adaptive solutions to boundary-value problems. Math. Comp. **31**, 333–390 (1977)
4. Dendy, J.E. Jr.: Black box multigrid. J. Comp. Phys. **48**, 366–386 (1982)
5. Dendy, J.E. Jr., Ida, M.P., Rutledge, J.M.: A semi-coarsening multigrid algorithm for SIMD machines. SIAM J. Sci Stat. Comput. **13**, 1460–1469 (1992)
6. Dendy, J.E. Jr., McCormick, S.F., Ruge, J.W., Russell, T.F., Schaffer, S.: Multigrid methods for three-dimensional petroleum reservoir simulation. In: 10th Symposium on Reservoir Simulation, Houston, pp. 19–25. Society of Petroleum Engineers (SPE), Inc. February 6–8 (1989)
7. Eliasson, P.: Dissipation Mechanisms and Multigrid Solutions in a Multiblock Solver for Compressible Flow. PhD thesis, Royal Institute of Technology, Stockholm, Sweden (1993)
8. Engquist, B., Osher, S.: Stable and entropy satisfying approximations for transonic flow calculations. Math. Comp. **34**, 45–75 (1980)
9. Ferm, L., Lötstedt, P.: Two-grid solution of shock problems. SIAM J. Sci. Comput. **18**, 1533–1552 (1997)

10. Godunov, S.K.: Finite-difference method for numerical computation of discontinuous solutions of the equations of fluid dynamics. Mat. Sbornik **47**, 271–306 (1959)
11. Grasso, F., Marini, M.: Solutions of hypersonic viscous flows with total variation diminishing multigrid techniques. Comput. Fluids **24**, 571–592 (1995)
12. Gustafsson, B., Lötstedt, P.: Analysis of the multigrid method applied to first order systems. In Mandel, J., et al. (ed.) Proceedings of the Fourth Copper Mountain Conference on Multigrid Methods, pp. 181–233. SIAM Philadelphia, PA (1989)
13. Hackbusch, W.: Multi-grid methods and applications. Springer, Berlin Heidelberg New York (1985)
14. Hall, M.G.: Cell vertex multigrid schemes for solution of the Euler equations. In IMA Conference on Numerical Methods for Fluid Dynamics, Reading (1985)
15. Hemker, P.W.: Multigrid methods for problems with a small parameter. In: Griffiths, D.F. (ed.) Proceedings, Dundee, June–July 1983, Lecture Notes in Mathematics 1066, pp. 106–121. Springer, Berlin Heidelberg New York (1983)
16. Hemker, P.W., Johnson, G.M.: Multigrid approaches to the Euler equations. In: McCormick, S. (ed.) Multigrid Methods, pp. 57–72. SIAM, Philadelphia (1987)
17. Jameson, A.: Unpublished manuscript
18. Jameson, A.: Solution of the Euler equations for two dimensional transonic flow by a multigrid method. Appl. Math. Comp. **13**, 327–355 (1983)
19. Jespersen, D.C.: Recent developments in multigrid methods for the steady Euler equations. In Lecture notes for lecture series on computational fluid dynamics. von Karman Institute for Fluid Dynamics, Rhode–St.–Genese, Belgium (1984)
20. Jespersen, D.C.: A time-accurate multiple-grid algorithm. AIAA paper 85-1493-CP (1985)
21. Koren, B., Hemker, P.W.: Damped, direction-dependent multigrid for hypersonic flow computations. Appl. Numer. Math. **7**, 309–328 (1991)
22. Leclercq, M.P., Stoufflet, B.: Characteristic multigrid method application to solve the Euler equations with unstructured and unnested grids. J. Comput. Phys. **104**, 329–346 (1993)
23. LeVeque, R.: Numerical Methods for Conservation Laws. Birkhäuser, Zürich (1992)
24. Lötstedt, P., Gustafsson, B.: Fourier analysis of multigrid methods for general systems of PDEs. Math. Comp. **60**, 473–493 (1993)
25. Mulder, W.: A new multigrid approach to convection problems. J. Comp. Phys. **83**, 303 (1989)
26. Mulder, W.A.: Multigrid for the one-dimensional invscid burgers equations. SIAM J. Sci. Comput. **11**, 33–50 (1990)
27. Ni, R.H.: A multiple-grid scheme for solving the Euler equations. AIAA **20**, 1565–1571 (1982)
28. Reusken, A.: Multigrid with matrix-dependent transfer operators for a singular perturbation problem. Computing **50**, 199–211 (1993)
29. Ruge, J.W., Stüben, K.: Algebraic multigrid. In: McCormick, S. (ed.) Multigrid Methods, pp. 73–130. SIAM, Philadelphia (1987)
30. Smith, R.A., Weiser, A.: Semicoarsening multigrid on a hypercube. SIAM J. Sci Stat. Comput. **13**, 1314–1329 (1992)
31. Spekreijse, S.: Multigrid solution of monotone second-order discretization of hyperbolic conservation laws. Math. Comput. **49**, 135–155 (1987)
32. Tang, W.P., Wan, W.L.: Sparse approximate inverse smoother for multi-grid. SIAM J. Matrix Anal. Appl. **21**, 1236–1252 (2000)
33. Wesseling, P.: An Introduction to Multigrid Methods. Wiley, Chichester (1992)
34. Wittum, G.: On the robustness of ilu smoothing. SIAM J. Sci. Stat. Comput. **10**, 699–717 (1989)
35. Xu, J.: Iterative methods by space decomposition and subspace correction. SIAM Review **34**, 581–613 (1992)
36. De Zeeuw, P.M.: Matrix-dependent prolongations and restrictions in a blackbox multigrid solver. J. Comp. Appl. Math. **33**, 1–27 (1990)